Biophysical Chemistry 20 (1984) 81–87
Elsevier

BPC 00856

A MICELLE MODEL FOR THE SEDIMENTATION BEHAVIOR OF BOVINE β-CASEIN

Mei-sheng TAI and Gerson KEGELES *

Section of Biochemistry and Biophysics, The Biological Sciences Group, The University of Connecticut, Storrs, CT 06268, U.S.A.

Received 24th October 1983
Accepted 12th December 1983

Key words: Key words: Sedimentation velocity; β-Casein; Micelle model

The monomer-single polymer model of G.A. Gilbert (Disc. Faraday Soc. 20 (1955) 68) for moving boundary sedimentation has been used by Payens and colleagues to explain the observed results for bovine caseins, and by Harrington and colleagues to explain the observed results for myosin fibrils. Electron microscope pictures of Buchheim and Schmidt have subsequently revealed micellar β-casein in the form of slightly elongated or spherical particles having a bimodal size distribution, but with a broad range of particle sizes, at concentrations not too far above the critical micelle concentration. The equilibrium properties of a broadly distributed micellar system can be fitted by the shell model developed by one of us, and in the present article, the shell model is extended to predict the moving boundary sedimentation behavior of such a system. The observed sedimentation patterns, as well as the critical concentration predictions of the monomer-single polymer Gilbert sedimentation model, are satisfactorily described with the present model, based on a continuous distribution of intermediates between monomers and the largest possible spherical micelles. For one example considered, the predicted frequency distribution of molecular weight is in qualitative agreement with the frequency distribution of particle volume found by Buchheim and Schmidt.

1. Introduction

In 1955 Gilbert [1], in a breakthrough in the understanding of the sedimentation analysis of self-interacting protein systems, showed that Schlieren optical resolution of moving boundaries should be expected for polymers above dimer, in a monomer-single polymer rapidly equilibrating mixture. In a subsequent paper [2], diminished resolution was predicted to be still attainable, in favorable situations, in the case of a series of close intermediates. The monomer-single polymer model [1], which predicts a critical concentration below which no 'polymer' sedimentation boundary is formed, and above which the slow 'monomer' boundary peak remains constant in size and velocity, independent of increasing total concentration, is precisely a transport analysis of the classical monomer-single high polymer 'two-state' model of micellization. Just as that single high polymer model can serve as an equilibrium approximation to the true picture of a size distribution containing a broad range of intermediates at low concentration [3], so the transport model [1] of monomer-single high polymer has been used [4,5] to explain the sedimentation behavior of protein micellar systems. The micellar nature of solutions of highly purified caseins has been definitively proven in experimental studies [5]. The corollary of Gilbert's predictions for a monomer-single polymer analysis has been often assumed as true; i.e., that a system exhibiting the predicted behavior must contain a monomer and single polymer in equilibrium. In the case of bovine β-casein, recent electron microscope studies [6] have revealed considerable breadth in the actual particle size distribution. It is the purpose of the present study to demonstrate that a different transport model, based on the shell model for micelles [7], predicts the observable

* To whom correspondence should be addressed.

sedimentation pattern resolution quite well, and still reproduces the interesting micellar type of critical concentration behavior originally predicted by the Gilbert theory [1] for the sedimentation of a monomer-single high polymer system. In consequence, it is not necessary to assume the existence of only a single high polymer in order to explain the observed resolution in moving boundary sedimentation of micellar proteins. Protein micellar systems showing such resolution should be examined by other techniques in addition to sedimentation [6], to test for the possible existence of a broad range of appreciable concentrations of intermediates centered about some large mean degree of polymerization. It is interesting that a classical statistical mechanical analysis of micellar equilibria [8] also predicted a broad distribution of intermediates.

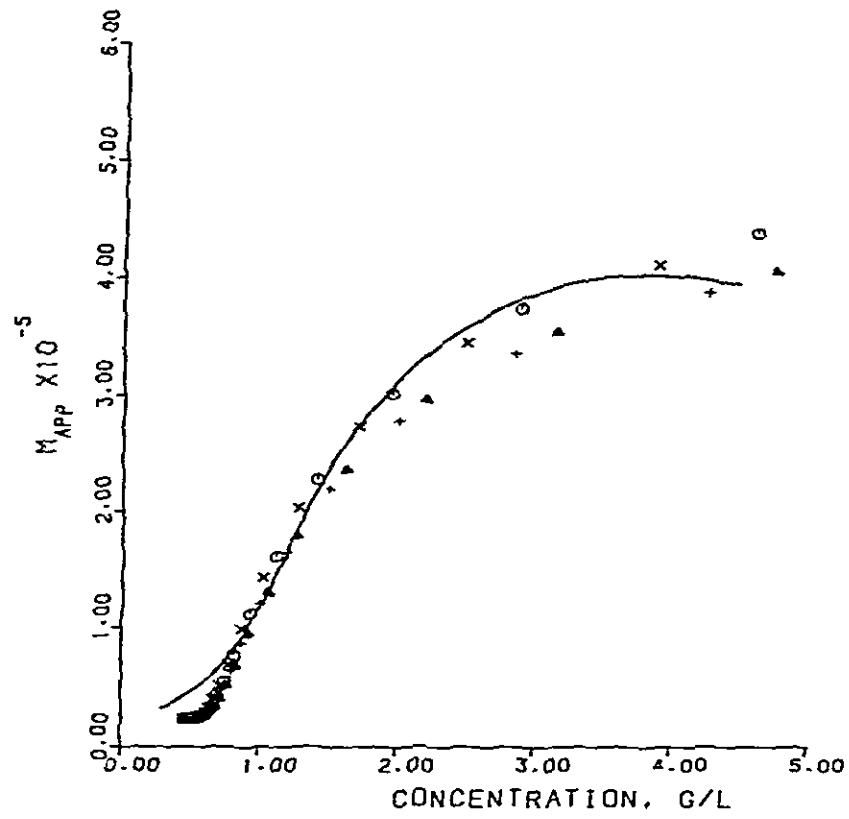

Fig. 1. Concentration dependence of the apparent weight-average molecular weight of β-casein sample 'Josje 2'. Solid lines are as measured by light scattering. Experimental conditions: phosphate buffer (pH 7.0). $I = 0.2$ (measured by Dr. B.W. van Markwijk of the National Institute for Dairy Research, Ede, The Netherlands). Points are calculated from the shell model for four sets of selected values of n and f. (⊙) $n = 46$, $f = 2\times10^{-4}$; (×) $n = 46$, $f = 3\times10^{-4}$; (△) $n = 40$, $f = 2\times10^{-4}$; (+) $n = 40$, $f = 3\times10^{-4}$.

2. Equilibrium properties

Two samples of bovine β-casein were very kindly supplied to us by Dr. T.A.J. Payens of the National Institute for Dairy Research, Ede, The Netherlands, for the kinetic studies presented in the companion article [9]. His brief description of the samples is reproduced in the companion article. The dependence of the light scattering on concentration for the two samples was also kindly furnished us, as measured by Dr. B.W. van Markwijk, and the results for the best sample are shown in fig. 1. In the shell model [7] equilibrium distribution of micelles, three essential parameters are required to describe the system: the maximum possible degree of polymerization, n, the intrinsic formation constant, K, and the (anti) nucleation factor, f, opposing the formation of a dimer from two monomers. The dimer at greatly reduced concentration acts as the nucleus for the formation of all higher polymers. The equivalent concentration ratio of any species, A_i, to that of monomer, A_0, is given [7] by eq. 1:

$$(i+1)[A_i]/[A_0] = f\frac{n!}{(n-i)!}\left(\frac{K[A_0]}{n}\right)^i \qquad (1)$$

A large number of trial values were selected for these parameters to try to fit the observations in fig. 1, the predicted weight average molecular weight from the shell model of eq. 1 being taken as proportional to the observed light scattering, with no correction for nonideality. As nonideality causes the measured curve to turn downward at sufficiently high concentrations [10], greater weight has been attached to the quality of the theoretical fit at low concentrations. In fig. 1 are also shown points calculated from the shell model for four sets of selected values of n, K and f. The range of values for which good fits were obtained is quite narrow.

One procedure for narrowing the choice of these parameters is as follows. The theoretical condition [7] for the incipient emergence of a polymer peak in the molar micellar distribution relates the maximum micellar size, n, to the product of the intrin-

sic equilibrium constant and the monomer concentration, according to the equation:

$$K[A_0] = n/(\sqrt{n+2} - 1)^2 \quad (2)$$

The value of the so-called propagation coefficient, $K[A_0]$, under the conditions of eq. 2 is that corresponding to the critical micelle concentration, CMC. Given this value of $K[A_0]$ in eq. 2, one can assume a value of f (eq. 1) and then calculate the relative concentration [7], $CMC/[A_0]$, which, according to the shell model, is always somewhat larger than unity. With a series of $CMC/[A_0]$ values, each for an assumed f value, thus derived from experimental estimates of n, one can compute corresponding values of $[A_0]$ and K with the aid of experimental CMC values. Each selection of a choice of f and K will be individually consistent with the experimentally derived estimates of n and CMC. However, each separate combination of f and K so chosen will also lead to a somewhat different prediction for the overall dependence of the weight-average molecular weight on total equivalent concentration. Final estimates for these parameters are then based on the most satisfying predicted fit to the experimental data shown in fig. 1. It should be emphasized that the experimental maximum micellar size shown in fig. 1 gives a degree of polymerization about one-half that of the maximum possible size, n (i.e., the size distribution centers about $n/2$ for virtually complete micellization [7], in which state the ratio of weight-average to number-average degrees of polymerization, excluding monomers, is very near unity [3]).

3. The moving boundary sedimentation model

The moving boundary sedimentation behavior is simulated by means of the countercurrent distribution analog [11]. An immiscible (upper) moving phase is used as a hypothetical construct in order to provide for stepwise advance of all macromolecular solute species, 'sandwiched' between reequilibration steps. In the aqueous phase, reequilibration is required for every hypothetical 'tube', or location in the represented sedimentation column, according to the restrictions of the shell model (eq. 1). In order to allow continually increasing rates of sedimentation with degree of polymerization, an arbitrary schedule of partition coefficients, P_i, has been constructed. This gives a very approximate fit to the model that in spherical micelles showing no change of solvation with degree of polymerization, the sedimentation coefficient increases with the 2/3 power of the molecular weight. Thus, we have taken

$$P_i = 0.1 + 0.2i, \quad i = 0, 1, 2 \ldots n \quad (3)$$

The transport rate increases as $P_i/(1 + P_i)$ [12]. For $i = 50$, the sedimentation coefficient should be 13.6-times that of the monomer based on $M^{2/3}$. We note that the monomer is not spherical, however [5]. The ratio of $P_{50}/(1 + P_{50})$ to $P_0/(1 + P_0)$, according to eq. 3 is $(10.1/11.1;/(0.1/1.1)$ or 10.01. Experiments suggest that at low concentrations, the ratio of fast peak to slow peak sedimentation rates is approx. 10. At high concentrations, the sedimentation rate of the polymer peak slows a great deal [5]. Thus, the schedule given by eq. 3 should provide transport rates of roughly correct magnitudes. A set of different equilibrium constants for all the elementary reaction steps between oligomers and monomer must hold for the hypothetical upper mobile phase, but all of these are fixed by the equilibrium constant values in the aqueous (lower) phase and by the schedule of partition coefficients in eq. 3. Thus, when a solution in the lower phase containing monomer and micelles at a given concentration reaches equilibrium in the aqueous (lower) phase for all species, this requires an upper phase distribution of concentrations which is entirely fixed by the schedule of partition coefficients given in eq. 3. Prior to the simulated sedimentation, all tubes are loaded with 'plateau region' upper and lower phases at equilibrium. It is noted that, according to custom, all concentrations for the countercurrent distribution analog are taken in units of equivalent concentration per unit volume, putting them on the same scale as visualized by refractometric observation of sedimentation. For a given micellar species, A_i, at a molar concentration $[A_i]$ at equilibrium in the lower phase, the equivalent concentration being $(i + 1)[A_i]$, the total equilibrium equivalent con-

centration in both phases must be $(1 + P_t)(i + 1)[A_t]$ or, by eq. 3,

$$T_t = (1 + 0.1 + 0.2i)(i + 1)[A_t] \quad (4)$$

One additional aid to the computation should be described. When the total concentration in the lower phase is above the CMC, the equivalent concentration micellar distribution for species other than monomer becomes fairly symmetrical [7]. It is found that the equivalent concentration, by use of the Stirling approximation for large factorials, becomes nearly Gaussian,

$$(i + 1)[A_t]/[A_o] \approx f\frac{(K[A_0])^{n+1/2}}{e^{n(1-1/K[A_0])}} e^{-(K[A_0]/2n)x^2} \quad (5)$$

where x represents the distance, in units of degree of polymerization, between the i-mer and the position of the maximum in the distribution curve:

$$x = i - i_{max} = i - n(1 - 1/K[A_0]) - 1/2 \quad (6)$$

If one seeks the total relative equivalent concentration of micellar species, excluding monomer, this is obtained by integration of the Gaussian distribution function in eq. 5 from $x = -\infty$ to $x = \infty$, giving

$$\frac{C^0 - [A_0]}{[A_0]} = f\frac{(K[A_0])^n\sqrt{2\pi n}}{e^{n(1-1/K[A_0])}} \quad (7)$$

The results from eq. 7 at given values of f, $K[A_0]$ and n usually agree with the exact results obtained by summation of all equivalent concentrations from the shell model, to better than one part in 1000. It is much simpler and quicker, given a total concentration, to estimate the monomer concentration by successive approximation using eq. 7 than to do so by trial and error, summing over the whole shell model distribution containing n separate oligomer terms. Such summations converge quickly below the CMC using the whole shell model distribution. Above the CMC, they do not converge easily, and eq. 7 is used until convergence is obtained, by appropriately incrementing or decrementing $[A_0]$ or $K[A_0]$, after which a final slightly more exact estimate can be made quickly with the use of the whole shell model distribution. At each given total concentration, it is necessary to know the lower phase concentration of monomer and every oligomer, in order to compute the amount transferred. It should be mentioned that the present computation, because of its complexity, has used the rectangular cell, constant-field approximation of the countercurrent distribution analog, and has not taken into account pressure effects.

4. Moving boundary sedimentation behavior

Predicted sedimentation velocity patterns for bovine β-casein in the neighborhood of room temperature are shown in figs. 2, 3 and 4, for concentrations just below, a little above and well

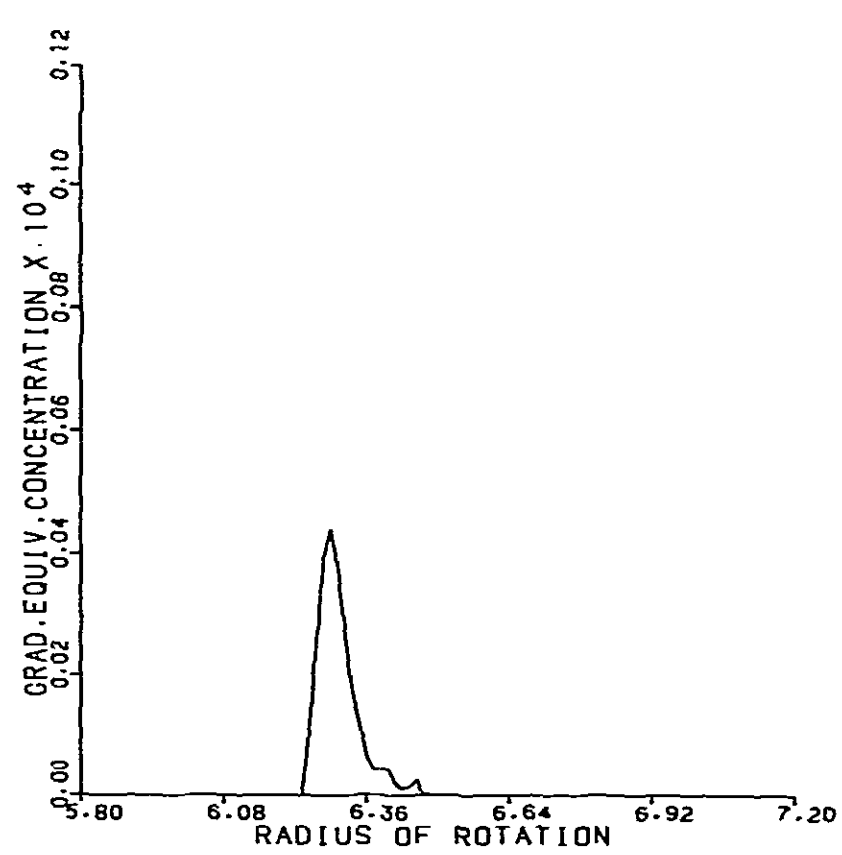

Fig. 2. Simulated concentration gradient sedimentation pattern of β-casein at 0.95×CMC using shell model. Conditions: $n = 46$, $f = 2.0\times10^{-4}$, CMC $= 2.55\times10^{-5}$ equiv./l, sedimentation at 40000 rpm. The pattern was computed for 50 transfers in countercurrent distribution analog. The initial position of the starting boundary was assumed to be 0.42 cm below the meniscus, at 6.22 cm, to correspond to synthetic boundary experiments.

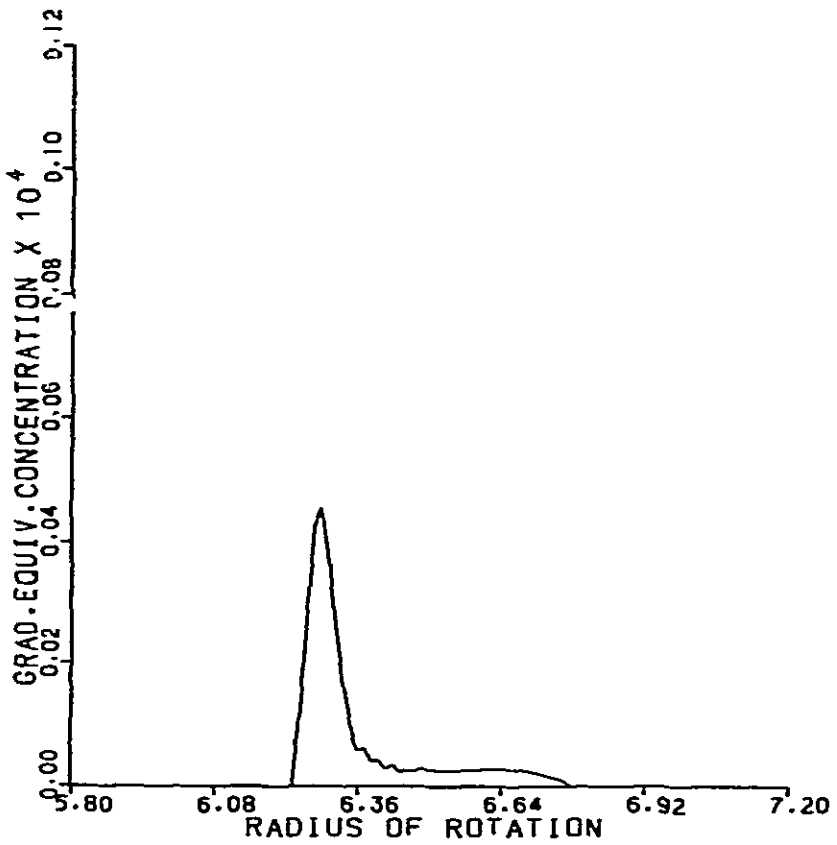

Fig. 3. Simulated concentration gradient sedimentation pattern of β-casein at 1.2×CMC. All other parameters as in fig. 2.

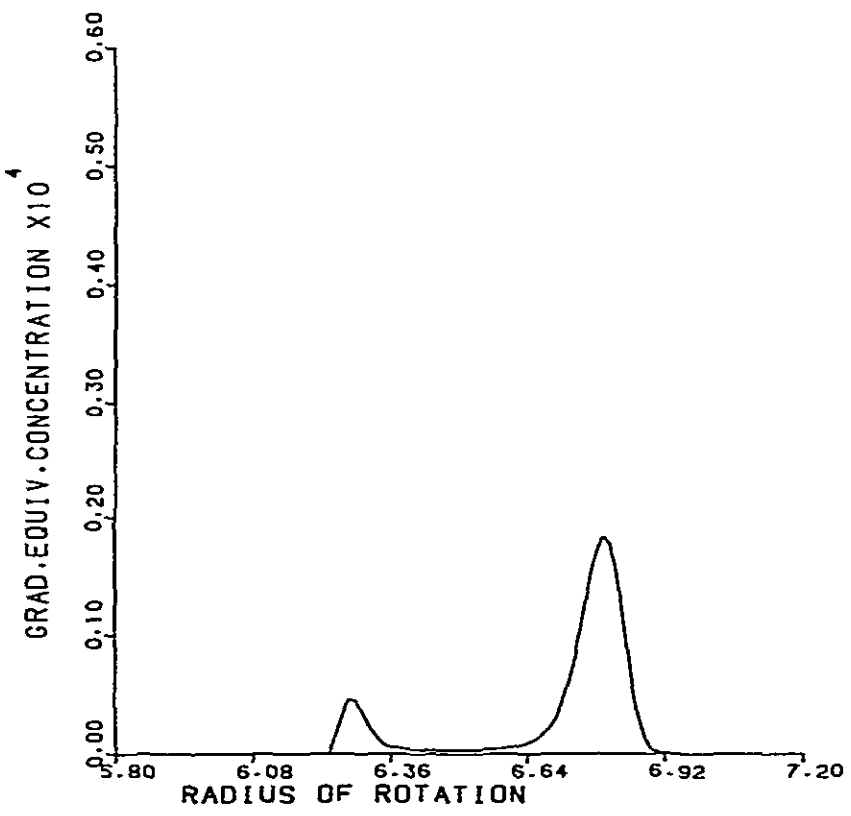

Fig. 4. Simulated concentration gradient sedimentation pattern of β-casein at 6.9×CMC (4.4 g/l). All other parameters as in fig. 2.

above the CMC, respectively. For these predictions, the value of n was chosen as 46 and the CMC was taken as 2.55×10^{-5} equiv./l at 20°C [13]. The value of f was taken as 2×10^{-4}. These choices are consistent with the information shown in fig. 1. The irregularities ahead of the slow peak are artifacts produced by cumulative error from the routine for computation of the monomer concentration. It is noted that the predictions are in accord with the results obtained at 20°C by Hoagland [14], which differ as expected from the sedimentation patterns published earlier by Payens and Van Markwijk [5] for temperatures of 8.5 and 13.5°C.

In order to compare these predictions with experiments for the particular samples in question at similar temperatures, sedimentation experiments were performed in a buffer consisting of 0.2 M phosphate at pH 7.0. The temperature was 20°C, the rotor speed 42040 rpm and, due to the small sedimentation coefficient of monomer and the very small CMC concentration, experiments were made in a 12 mm synthetic boundary cell. The results are shown in the sedimentation velocity Schlieren diagram in fig. 5. Comparison of fig. 4 with fig. 5 shows that the assumed shell model distribution, with the given choices of n, f and CMC, correctly predicts the experimental sedimentation behavior of β-casein micellar systems.

5. Equilibrium size distribution

With the choice of $n = 46$, $f = 2 \times 10^{-4}$ and CMC $= 2.55 \times 10^{-5}$ equiv./l, for phosphate buffer (pH 7) [13] at 20°C, the value of $K[A_0]$ required to reach any specified ratio of equivalent concentration to the CMC is computed as outlined above. To compare with the particle size distribution measured by Buchheim and Schmidt [6], at a concentration of 1.26 mg/ml at 22°C in ammonium acetate buffer at pH 7, it is assumed that the CMC is approximately the same as at pH 7 and 20°C, in phosphate buffer [13]. The predicted molar distribution as a function of degree of polymerization is shown in fig. 6. This distribution may be compared with that shown in fig. 1 of ref. 6 for particle volume frequency at a concentration

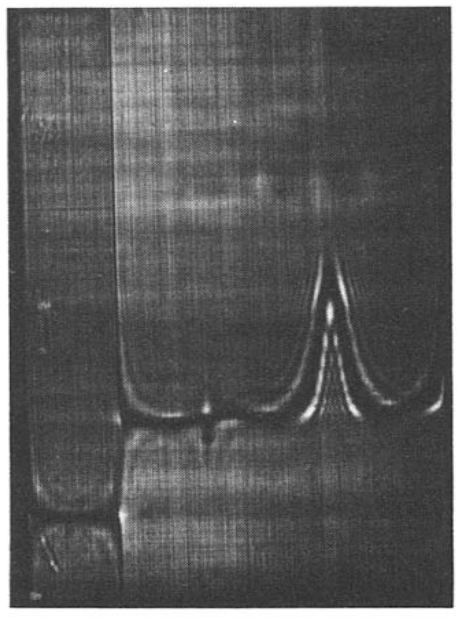

Fig. 5. Sedimentation pattern of β-casein sample Josje 2 (4.4 g/l) in phosphate buffer (pH 7.0, $I = 0.2$) at 20°C. Sedimenting in a synthetic boundary cell for 35 min at 42040 rpm. Phase plate angle 40°.

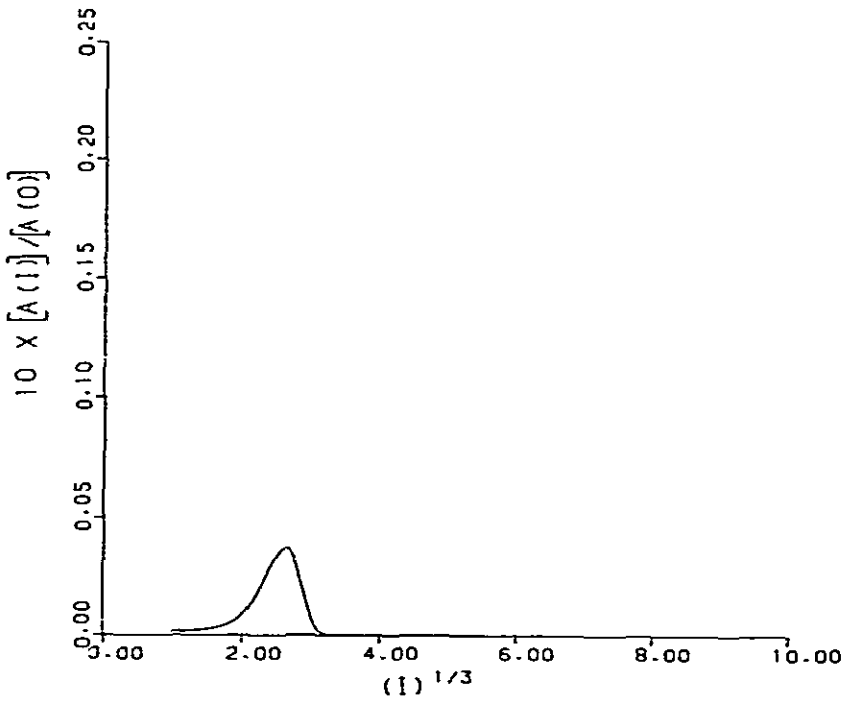

Fig. 6. The predicted relative molar distribution $[A_i]/[A_0]$ as a function of cube root of degree of polymerization $(i)^{1/3}$ using shell model. n-46. $K[A_0] = 1.717$. Monomer is at 1.0 relative concentration and dimer $= 0.5/K[A_0]$ in the plot. The value of $K[A_0] = 1.717$ was chosen to agree with the number average molecular weight of 45000 reported by Buchheim and Schmidt [6].

of 1.26 mg/ml. The shell model itself assumed that the variation of equilibrium constant with temperature or pressure would be the same for every elementary reaction. Thus, particle volume would become a linear function of degree of polymerization. The supposition of Buchheim and Schmidt [6] that molecular volume is directly proportional to molecular weight appears to be experimentally substantiated in their study. The qualitative comparison between fig. 6 and the distribution shown in fig. 1 of ref. 6 therefore suggests that the shell model offers a reasonable prediction for the micellization of β-casein under these conditions.

6. Discussion

Some of the originally startling predictions of the Gilbert theory [1] for a monomer-single polymer system were that no polymer peak would emerge until a critical concentration was reached, that above this concentration both the area under the slow Schlieren peak and the velocity of that peak would be unchanging with increasing concentration, and that both the area and the velocity of the faster peak would increase continually with increasing concentration. With appropriate hindsight, all of these properties are what one would now expect for the behavior of a classical two-state micellar system.

It is interesting to test the corresponding predictions of the current model. In fig. 7 are shown diagrams for predictions of the sedimentation patterns below, just at, and just above CMC. The irregularities ahead of the slow peak at the lower concentrations are artifacts produced by cumulative errors from the routine for computation of the monomer concentration. It is seen that, except as expected below the CMC, the 'monomer' peak is virtually invariant in size, shape and velocity, while the 'polymer' peak increases in size and slightly in velocity with increasing concentration. This requirement of the Gilbert monomer-single polymer model is therefore also fully met by the current model. In fact, for a micellizing protein system at a high degree of polymerization, it would be extremely difficult, if not impossible, by means of

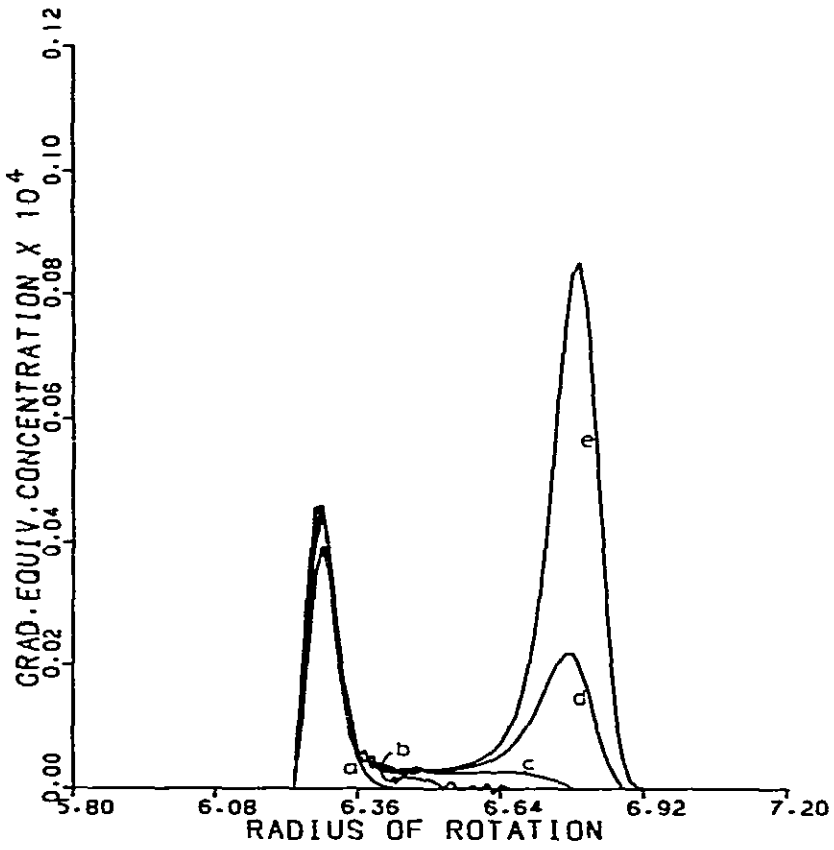

Fig. 7. Simulated concentration gradient sedimentation pattern of β-casein at different total concentrations: (a) 0.8×CMC, (b) CMC, (c) 1.2×CMC, (d) 2×CMC, (e) 4×CMC. The pattern was computed for 50 transfers in countercurrent distribution analog. All other parameters as in fig. 2.

sedimentation velocity experiments alone, to distinguish between a monomer-single high polymer model of the Gilbert theory and a continuous shell model distribution, with low concentrations of intermediates in a valley between monomer and micelles, the latter being distributed around some large mean particle size. Consequently, additional other methods, such as equilibrium ultracentrifuge experiments and electron microscope examination [6], should be employed to assess more fully the microscopic nature of a micellar protein system. It is especially important to emphasize that in spite of the assumed broad distribution of sizes, the polymer peak, once fully formed, hardly increases in velocity at higher concentrations. Moreover, excellent resolution is predicted between slow and fast sedimenting peaks.

One property of the bovine β-casein micelles which has not been fully explained is also not explained by the current model. This is the large reduction reported [5] in the sedimentation velocity of the fast peak at high concentrations. A possibility would be the formation of long rod-shaped micelles [3], but no indication of this formation was presented in intrinsic viscosity [5], electron microscope [6] or angular dependence of light scattering [13] studies. Another possibility suggested earlier by Payens and colleagues [15] was increased solvation and swelling of the micelles at high concentration. No effort has been made here to incorporate any hydrodynamic or other s on c dependence with the current model, except that caused directly by polymerization.

Acknowledgements

The authors are especially indebted to Dr. T.A.J. Payens and his colleagues at the National Institute for Dairy Research, Ede, The Netherlands, for a gift of two samples of purified bovine β-casein and for data on their light scattering versus concentration behavior. This work was made possible in part by a grant from The University of Connecticut Research Foundation.

References

1 G.A. Gilbert, Disc. Faraday Soc. 20 (1955) 68.
2 G.A. Gilbert, Proc. Soc. A250 (1959) 377.
3 P. Mukerjee, J. Phys. Chem. 76 (1972) 565.
4 R. Josephs and W.F. Harrington, Proc. Natl. Acad. Sci. U.S.A. 58 (1967) 1587.
5 T.A.J. Payens and B.W. van Markwijk, Biochim. Biophys. Acta 71 (1963) 517.
6 W. Buchheim and D.G. Schmidt, J. Dairy Res. 46 (1979) 277.
7 G. Kegeles, J. Phys. Chem. 83 (1979) 1728.
8 C.A. Hoeve and G.C. Benson, J. Phys. Chem. 61 (1957) 1149.
9 C. Huang, M. Tai and G. Kegeles, Biophys. Chem. 20 (1984) 89.
10 T.A.J. Payens, J.A. Brinkhuis and B.W. van Markwijk, Biochim. Biophys. Acta 175 (1969) 434.
11 J.L. Bethune and G. Kegeles, J. Phys. Chem. 65 (1961) 1761.
12 L.C. Craig and D. Craig, in: Technique of organic chemistry, ed. A. Weissberger, vol. III (Interscience, New York, 1950).
13 D.G. Schmidt and T.A.J. Payes, J. Colloid Interface Sci. 39 (1972) 655.
14 P.D. Hoagland, J. Dairy Sci. 49 (1966) 783.
15 T.A.J. Payens and H.J. Vreeman, in: Solution behavior of surfactants, vol. 1, eds. K.L. Mittal and E.J. Fendler (Plenum Press, New York, 1982) p. 543.